Molecular fingerprints of star formation throughout the Universe : a space-based infrared study

Lahuis, F.

Chapter 3

From Molecular Cores to Planet Forming Disks – a c2d data legacy –

Abstract

The *Spitzer* legacy program "From Molecular Cores to Planet Forming Disks" ("Cores to Disks" or c2d) was one of the five initial *Spitzer* legacy programs. The program included mapping and spectroscopy of the nearby Chamaeleon, Lupus, Perseus, Ophiuchus, and Serpens star-forming regions. High-S/N spectra have been obtained within the 5-38 μm range for 226 sources at all phases of star and planet formation up to ages of $\sim$5 Myr. This includes previously known young stars and new sources discovered in the IRAC and MIPS maps. The c2d program is complementary to the "The Formation and Evolution of Planetary Systems: Placing Our Solar System in Context" (FEPS) *Spitzer* legacy program. Together both programs covers stellar evolution from $0 - 3$ Gyr. Previous spectroscopic studies, e.g., with ISO, had the sensitivity to probe only high- or intermediate-mass young stellar objects. *Spitzer* permits the first comprehensive mid-infrared spectroscopic survey of solar-type young stars. This Chapter describes the c2d pipeline developed to reduce and analyse the IRS pointed observations. The c2d pipeline is also developed to prepare the IRS legacy products delivered to the *Spitzer* Science Center (SSC) for distribution to the general public.

Based on *Lahuis, F., Kessler-Silacci, J. E., Evans, N. J., II, Blake, G. A., van Dishoeck, E. F., Augereau, J.-C., Banhidi, Z., Boogert, A. C. A., Brown, J. M., Geers, V. C., Jørgensen, J. K., Knez, C., Merín, B., Olofsson, J., & Pontoppidan, K. M. 2006, "c2d Spectroscopy Explanatory Supplement," (Pasadena: Spitzer Science Center)*

3.1 Introduction

The c2d observing strategy is described in detail in Evans et al. (2003). The 75 hour c2d IRS program consists primarily of IRS (Houck et al., 2004) observations of point sources. A small portion of the observing time was dedicated to IRS spectral maps of the south-eastern Serpens molecular core (Banhidi & et al., 2007) and the Barnard 1 outflow. A number of followup mini-maps (see §5.2.2) were observed on a number of sources from the initial program. The mini-maps were intended to check for extended gas-phase emission lines and polycyclic aromatic hydrocarbon (PAH) emission around point-sources. High-S/N spectra were obtained within the 5–38 μm range (high resolution [R≈600] over the 10–37 μm range) for 226 sources at all phases of star and planet formation up to ages of ∼5 Myr. Additionally, the MIPS () spectroscopy mode ($\lambda = 52 - 100\mu$m with a spectral resolution $R = \lambda/\delta\lambda = 15 - 25$) was used in the second year of the program to characterize the longer wavelength silicate and ice features of a small subsample of disks.

The c2d IRS program was divided into two sets with roughly equal time, the first-look (with the *Spitzer* observation program number (PID) #172) consisting of observations of known embedded, pre-main-sequence stars, and background stars and the second-look (PID #179) consisting of IRS follow-up spectroscopy of sources discovered in the IRAC and MIPS mapping surveys (Harvey et al., 2006; Jørgensen et al., 2006; Brooke et al., 2007; Rebull et al., 2007; Porras et al., 2007). The source list for the first-look program was restricted primarily to low-mass young stars, defined as having masses $M < 2\ M_{\odot}$, with ages younger than ∼5 Myr, for minimal overlap with existing infrared spectroscopy. Within these criteria, the selection contains a broad representative sample of young stars with ages down to 0.01 Myr and masses down to the hydrogen-burning limit or even less. The second-look IRS campaign was more focused on observations of new or interesting types of sources. The new sources were selected from the catalogues generated from the c2d IRAC and MIPS maps (PID 174, 175, 176, 177, and 178). Included in the second-look campaign are IRS staring observations of samples of very low-mass stars and brown dwarfs, weak-line T Tauri Stars, edge-on disks, very low luminosity objects (VeLLOs), and cold disks, as well as IRS mapping observations of extended outflows and followup mini-maps of extended gas-phase and PAH emission and 4 MIPS SED observations of interesting targets from the first-look campaign.

Almost all first-look targets were observed using the IRS staring mode in each of its four modules as listed in Table 3.1. The longest wavelength ends of SL1 and LL1 suffer from light leaks from higher orders and are therefore removed from the delivered spectra. For those sources that are part of various GTO programs involving the low-resolution modules, only the high-resolution 10–37 μm (SH,LH) spectra were acquired as part of the c2d IRS effort. In contrast to the scheduled *Spitzer* guaranteed time program observations (GTO) of large numbers of young stars, typically with the low-resolution IRS modules, the c2d IRS program focuses on long integration times in the high resolution modules, ensuring high dynamic range even on weak sources. For all first-look observations, the integration times for the short-high and long-high modules were fixed such that theoretical S/Ns of at least 100 and 50 were obtained for sources brighter and fainter than 500 mJy on the continuum, respectively. The spectra taken using the short-low modules always reach theoretical S/Ns of greater than 100. Second-look IRS staring targets were observed in various modules depending on the

Table 3.1. *Spitzer* IRS observing modules

Module	Wavelength range (μm)	Resolving power $R = \lambda/\delta\lambda$
SL1	$7.4 - 14.5$	$60 - 120$
SL2	$5.2 - 8.7$	$60 - 120$
LL1	$19.5 - 48.0$	$60 - 120$
LL2	$14.0 - 21.3$	$60 - 120$
SH	$9.9 - 19.6$	600
LH	$18.7 - 37.2$	600

SL1 and LL1 cover spectral order 1; SL2 and LL2 cover spectral order 2 and 3; SH and LH cover spectral orders 11 to 20.

source type and flux. S/Ns greater than 100 were achieved where possible, but since second-look consisted of primarily very weak sources, this was not always feasible. A full listing of all c2d IRS targets including observation details is included in the c2d IRS explanatory supplement[1] (Lahuis et al., 2006a).

As part of the second-look program, followup mini-maps of extended gas-phase and PAH emission around point source targets were taken using the IRS mapping mode. In addition, IRS spectral maps of the south-eastern Serpens molecular core and the Barnard 1 outflow were obtained. The Serpens molecular core was imaged over more than 7 arcmin^2 to a 1σ sensitivity of 2 mJy using the low-resolution IRS spectral mapping mode. This core contains several deeply embedded sources and possesses a complex physical structure with outflows on a scale of 30″–60″ ($\sim$0.05–0.1 pc) from the driving sources. The c2d IRS explanatory supplement gives details on the observing strategy, the IRS mapping reduction and the IRS mapping products provided included in the *Spitzer* legacy delivery.

To quickly assess the nature of the observed sources an automated feature identification of the most prominent spectral features is included in the c2d reduction pipeline and performed on all IRS staring observations and extracted spectra of individual map pointings. The identified features are listed in the product logfiles included in the legacy delivery. In the c2d IRS explanatory supplement master overview tables are included of all spectral features identified in the IRS spectra.

The MIPS SED observations taken as part of the second-look program were all "FixedSingle" observations, meaning that they were non-mapping, non-clustered AORs. The exposure time for all observations was 10 s, repeated as necessary to get S/N of 30–50 based on IRAS 60 μm and MIPS 70 μm fluxes and the 2004 sensitivity estimates for MIPS SED mode.

[1] The c2d IRS explanatory supplement can be downloaded from `http://ssc.spitzer.caltech.edu/legacy/c2dhistory.html` or `http://peggysue.as.utexas.edu/SIRTF/` under the menu item Data Products.

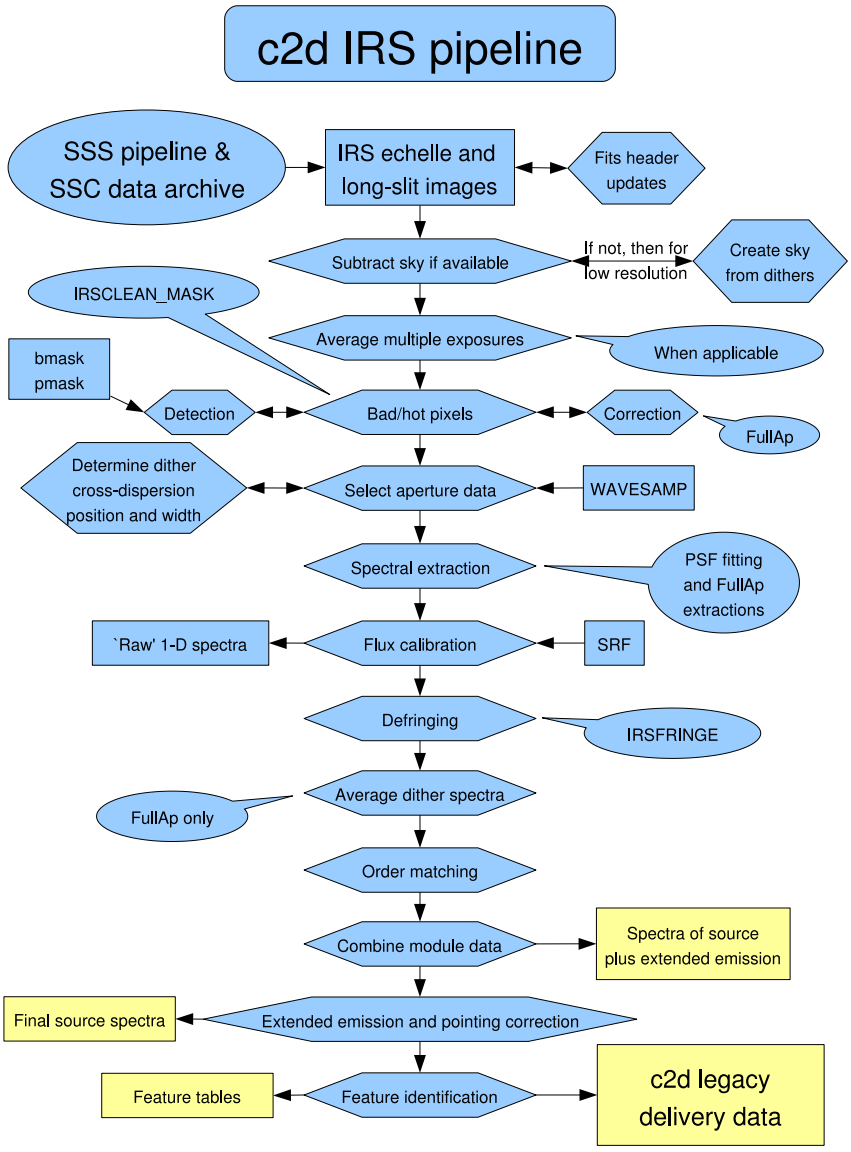

Figure 3.1 Schematic overview of the data reduction and legacy product generation for IRS staring mode observations in the c2d pipeline. Rectangles correspond data and products, polygons to tasks, and dialog baloons give short descriptions. The products in the white boxes are part of the c2d legacy delivery to the SSC. The data reduction process and products are described in detail in § 3.2 and § 3.3.

3.2 Reduction of IRS pointed observations

The *Spitzer* archive products include Basic Calibrated Data (BCD; *_bcd.fits) files, which are two dimensional spectra that have been processed through the SSC pipeline as described in the IRS data handbook[2]. This process entails saturation flagging, dark-current subtraction, linearity correction, cosmic ray correction, ramp integration, droop correction, stray light removal or crosstalk correction, and flat-field correction.

The IRS reduction starts from the intermediate RSC products (*_rsc.fits), which have had the stray light removed (for SL) or cross-talk corrected (for SH,LH) but no flat-field applied. LL has no known stray light issues and therefore no corrections are made. In our reduction, 1-D spectra are extracted from the long-slit (SL,LL) and echelle (SH,LH) images using two extraction methods (see § 3.2.2). The first is a full aperture extraction (§ 3.2.2.1) from images in which known bad/hot pixels have been corrected (see § 3.2.1). The second is an optimal PSF extraction (§ 3.2.2.2) based on fitting an analytical cross dispersion point spread function plus extended emission (assumed to be uniform over the adopted extraction aperture) to all non bad/hot image pixels (see § 3.2.1). The optimal PSF extraction uses an analytical fit to the good pixels only, and therefore bad/hot pixel correction is not required. The 1-D spectra for both extraction methods are flux calibrated using dedicated spectral response functions (SRFs) derived from a suite of calibrator stars using Cohen templates and MARCS models provided by the *Spitzer* Science Center (Decin et al., 2004). After extraction, the 1-D spectra are corrected for instrumental fringe residuals (see § 3.2.6) and, finally, an empirical order matching is applied (see § 3.2.7). For all extracted spectra, a log file, overview plot and an IPAC spectral table are generated. In the log file a list of the strongest spectral features is given (see § 3.3.9).

The c2d pipeline incorporates routines from SMART[3] (Higdon et al., 2004), OSIA,[4] IRSFRINGE,[5] and IRSCLEAN_MASK.[6] The pipeline also uses advanced reduction tools and calibration routines developed by the c2d and FEPS[7] legacy teams for full aperture extraction, optimal PSF extraction, automated product generation, and pointing correction (in development).

3.2.1 Bad/hot pixels

The '`pmask.fits`' and '`bmask.fits`' files provided by the SSC contain masks for permanently bad IRS array pixels ('hot' pixels), pixels affected by cosmic rays or full saturation, and a number of pixels with long-term transients as a result of solar flares or cosmic ray hits. The SSC pipeline interpolates over undefined pixels (pixels with the signal value 'NaN') in the images and ignores pixels flagged as fatal in the raw

[2] `http://ssc.spitzer.caltech.edu/irs/dh`

[3] `http://ssc.spitzer.caltech.edu/postbcd/smart.html`

[4] OSIA is a joint development of the ISO–SWS consortium. Contributing institutes are SRON, MPE, KUL and the ESA Astrophysics Division. `http://sws.ster.kuleuven.ac.be/osia/`

[5] IRSFRINGE is developed for the *Spitzer* science community by the "Cores to Disks" c2d legacy team. IRSFRINGE has been integrated into SMART but is also available as a stand-alone package from `http://ssc.spitzer.caltech.edu/postbcd/irsfringe.html`

[6] The IRSCLEAN_MASK software was developed by the IRS Instrument Support Team at SSC in conjunction with the Cornell IRS Science Center. It can be retrieved from `http://ssc.spitzer.caltech.edu/archanaly/contributed/irsclean/`

[7] See `http://ssc.spitzer.caltech.edu/legacy/fepshistory.html` for the FEPS Data Explanatory Supplement.

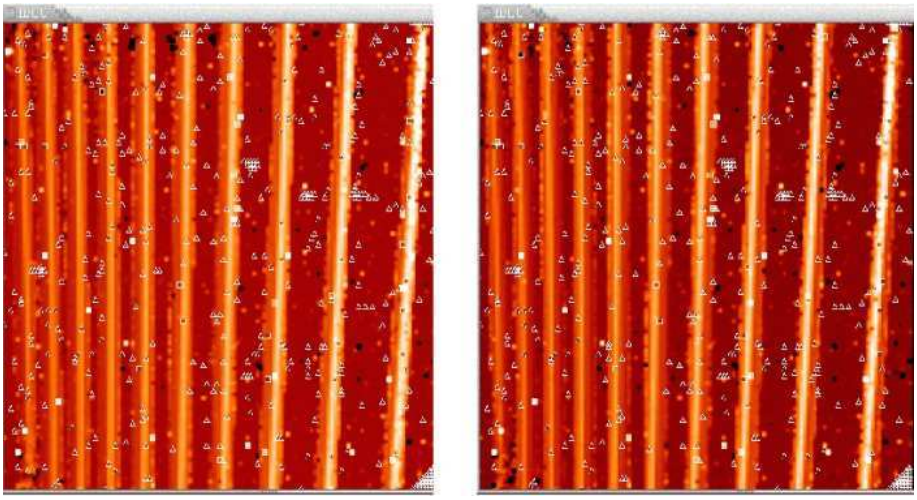

Figure 3.2 Two-dimensional BCDs of two dither positions in the LH module. Triangles and squares denote bad pixels, most of which are defined in the SSC bad pixel ('`pmask and bmask`') files.

SSC pipeline. In our reduction, an attempt is made to identify additional bad pixels in the optimal PSF extraction, and to correct all known bad pixels for the full aperture extraction.

The LH array is particularly affected by bad or hot pixels (see Figure 3.2). Although only $\lesssim 7\%$ of the pixels in LH are affected, collapsing the spectra along the spatial dimension of the slit during the extraction process results in $\sim$20% of the final spectral data points being affected. In reality, this number may be much larger, as the SSC mask files do not identify all transient, or 'hot' pixels, particularly at wavelengths > 30 μm. Correction of the identified bad pixels significantly improves the extracted spectra (Figure 3.3), but artifacts remain. In the SL, SH and LL modules the problem is much less severe but still requires attention as artifacts resulting from bad pixels may still be present.

It is particularly important to identify as many bad pixels as possible which fall within the extraction window before the 2-D data are processed into 1-D spectra to limit the number of possibly affected sprectral samples in the 1-D spectra. These include the hot pixels identified by the `pmask.fits` files and bad pixels identified by the BCD pipeline that are included in the `bmask.fits` files. The latter includes pixels affected in the data acquisition and pixels for which the calibration or reduction in the BCD pipeline failed. Aside from the known bad/hot pixels, additional affected pixels are identified using the IRSCLEAN_MASK program provided by the *Spitzer* Science Center.[8] A detailed description of the SSC pipeline processing is given in the IRS handbook[9].

After identifying as many bad pixels as possible, the c2d pipeline interpolates over the bad pixels for the full aperture extraction and ignores the bad pixels for the optimal PSF extraction. Specifically, the bad pixel correction is done by interpolating

[8] `http://ssc.spitzer.caltech.edu/archanaly/contributed/irsclean/`
[9] `http://ssc.spitzer.caltech.edu/irs/dh`

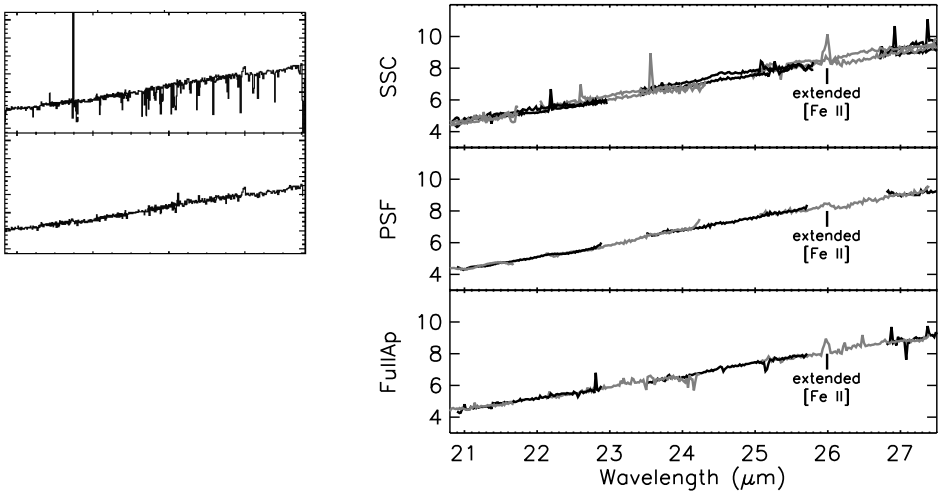

Figure 3.3 IRS LH spectra of IRAS 08242-5050 (HH46) affected by bad pixels. IRAS 08242-5050 was one of the legacy test cases observed directly after the in-orbit checkout. The first spectra produced by the SSC pipeline proved to be of poor quality as a result of the many LH bad pixels. The small plot shows the early archive spectrum in the top panel and one of the first c2d attempts at an optimal extraction in the lower panel. The right panel shows the current SSC pipeline and both c2d extractions (see § 3.2.2). The quality has improved significantly, however it is clear that artifacst resulting from bad pixels may still be present. The IRAS 08242-5050 spectrum also illustrates the appearance of extended emission lines between the PSF extraction and both full aperture extractions. The difference in strength reflects the difference between the IRS beam and the IRS aperture (see § 3.3.3).

over the bad pixels in the cross-dispersion direction for all apertures as defined by the `wavesamp` calibration file in the former case. The optimal PSF extraction profile is used as the interpolation function (see § 3.2.2.2). Significant improvement in data quality for both the SH and LH modules is thus achieved. (See Figure 3.3 for the result of the c2d bad pixel correction on part of a LH spectrum).

3.2.2 Spectral extraction

Once the bad/hot pixels have been corrected, the spectra are extracted using a full aperture or optimal PSF extraction. Prior to extraction, the c2d pipeline averages the RSC images of each dither position. For the full aperture extraction, 1-D spectra are extracted for each dither position, which are combined after correction for the spectral response function. For the optimal PSF extraction, both dither positions are combined and one single 1-D spectrum is extracted. This gives the best overall noise reduction and spectral stability, as is required for automated pipeline processing. Averaging before extraction also has the added benefit that missing pixels in one single image will be corrected for by good data in the other exposures.

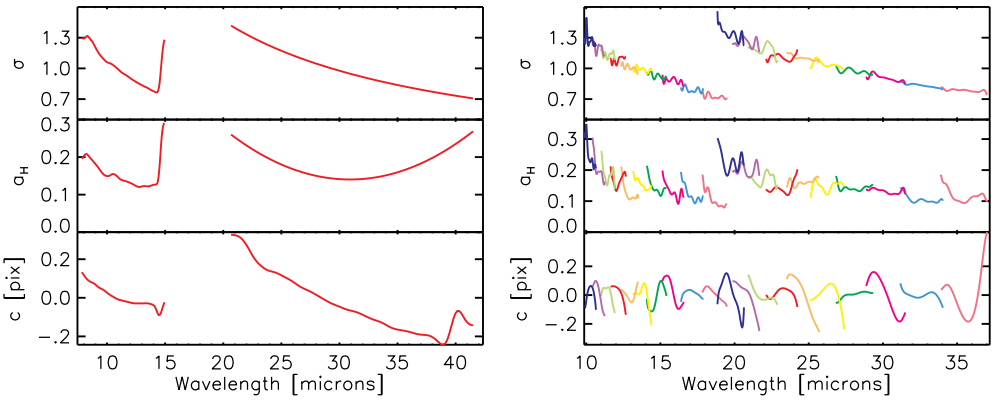

Figure 3.4 Parameters defining the IRS SL1, LL1, SH, and LH cross dispersion profiles for unresolved sources. The variation with wavelength within each order is, for high signal to noise calibrators, consistently reproduced from observation to observation and assumed to be real. These most likely result from mechanical and optical defects in the instrument.

3.2.2.1 Full aperture extraction

The first method of extraction employed in the c2d pipeline for both the low resolution and high resolution modules is similar to that employed in the SSC pipeline. The main difference is that the c2d pipeline performs a fixed-width aperture extraction from RSC products and then corrects for a spectral response function (SRF), while the SSC pipeline performs a varying aperture extraction from flat-field corrected BCD products. For the low resolution modules, the c2d pipeline implements an extraction aperture with a fixed width in pixels over the whole order. The source position in the slit is determined and the extraction aperture is centered on the source. The width is sufficiently wide that 99% of the flux of a point-source falls within the window. For the high resolution modules, the full slit width is used in the extraction. Figure 3.3 gives an example of a full aperture correction without and with bas-pixel correction.

The spectra are extracted separately for each dither position and later averaged into one single spectrum, with weights inversely dependent on the error.

For low resolution staring observations, the dither positions are used for the sky correction. For the high resolution modules, a sky estimate for the full aperture extraction is derived using the optimal PSF extraction method.

3.2.2.2 Optimal PSF extraction

Optimal extraction is performed on the combined RSC data after correcting for the cross dispersion offsets of the separate dither position images. The observed signal is assumed to be that of a point-source or slightly resolved source plus a uniform zero level (over the IRS extraction aperture). The zero level will in most cases represent the local extended emission close to the source, but it may also contain residuals of e.g., the raw pipeline dark current subtraction (see also § 3.3.3).

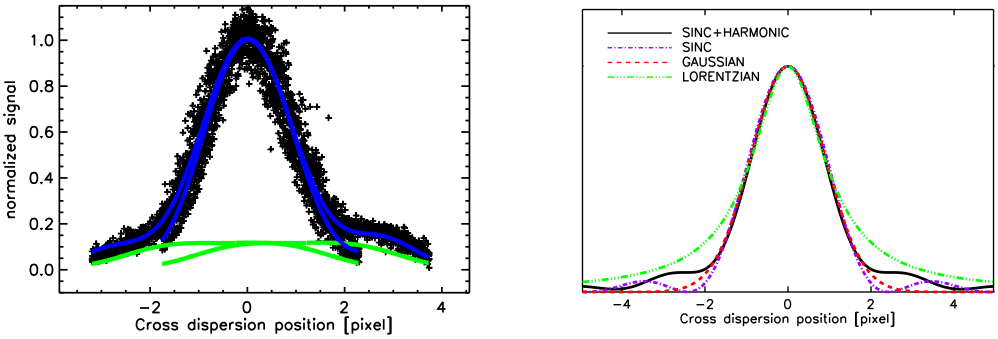

Figure 3.5 Example of the cross dispersion profile. The left plot shows a fit to the collapsed and cross-dispersion position corrected data (black pluses) from both dither positions of SH order 11 for GW Lup (see also Figure 3.8). The blue lines denote the source profile plus extended emission (green) for each dither position. The variations between the two dither positions reflect the flat-field profile of the zero level at the uncorrected slit position. The right plot shows a comparison of the IRS profile for a given width (σ) and harmonic amplitude compared to an undistorted sinc, a Gaussian, and a Lorentzian profile with the same FWHM. Note the significant variation in the strength and shape of the profile wings. The correct characterization of both the width and the wings of the profile is essential for reliably separating the compact source and extended emission components in the extraction.

3.2.3 The IRS cross dispersion PSF

Sky corrected high signal-to-noise calibrator data are used to define the IRS point spread function (PSF) in the cross dispersion direction. From these the detailed profile characteristics, the width of the profile, the offsets with respect to the pre-orbit definition of the order-traces, and the amplitude of the harmonic distortions are retrieved.

The IRS cross dispersion profile is approximated by the analytical function S;

$$S(x,\lambda) = \mathrm{sinc}^2(\sigma(\lambda) \times (x - c(\lambda))) + a_H(\lambda) \times H1(\lambda) + a_H(\lambda)^2 \times H2(\lambda).$$

The sinc width σ relates to the $FWHM$ by $\sigma = e/(2 * FWHM)$, c is the location of the profile center, more specifically the offset of the observed profile with respect to the pre-orbit defined order-trace, $H1$ and $H2$ are the first and second even harmonics (sinc overtones), and a_H the harmonic amplitude. The σ, c, and a_H wavelength dependence is shown in Figure 3.4. For SL and LL orders 2 and 3 the PSF is poorly defined as a result of spatial undersampling in the cross dispersion direction. For the extended emission within the aperture, the flat field cross-dispersion profile (describing the extended emission sensitivity) is used. The IRS flat fields have been derived by the *Spitzer* Science Center.

When applied to an individual observation, the cross dispersion offset of the trace and a scale factor for the width (for slightly extended sources) are determined from the collapsed order data (see Figure 3.5). Subsequently the 1-D spectra are extracted for all apertures defined in the IRS wavelength description (WAVESAMP) files. The PSF profile is fit to the aperture data keeping all parameters, except the profile amplitude and the zero level, fixed. After the extraction, the 1-D spectrum is flux calibrated using the SRF described in § 3.2.4.

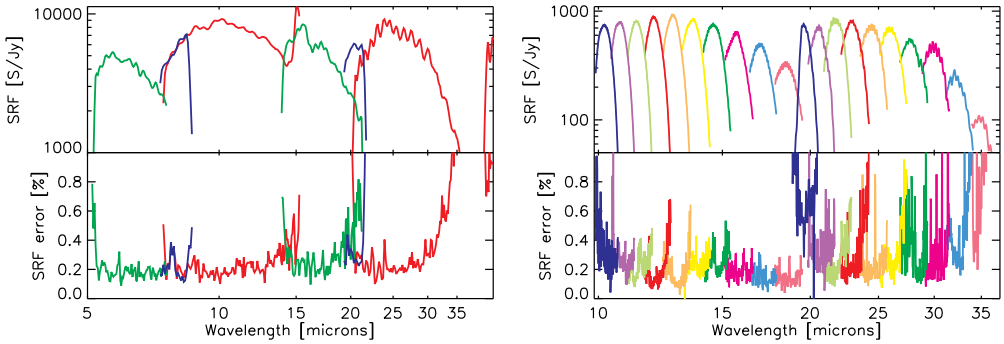

Figure 3.6 Spectral Response Function (SRF) for SH and LH for the optimal PSF extraction in units of S/Jy where S is the signal unit of the RSC echelle images. The orders are color coded, same for SH and LH. The SRF functions for the full aperture extraction show a similar profile and only change in detail and absolute level.

The advantages of PSF fitting are that it is less sensitive to bad data samples and unidentified bad pixels, that it gives an estimate of the data zero level and/or local sky contribution, and that it provides information on the extended nature of spectral features (see e.g. Geers et al., 2006).

The PSF fitting is sensitive to undersampling which can result in poorly defined continua. The short wavelength ends of the SH and LH modules suffer from this for some sources, but orders 2 and 3 of the SL and LL modules are most affected by undersampling. Therefore, we have chosen to include optimal extraction data only for the high resolution modules and for order 1 of the SL and LL modules. For the SL and LL order 2 and 3 data also no usable sky estimate can be obtained and these columns in the delivered IPAC tables contain zeros for these orders.

3.2.4 Spectral Response Function (SRF)

Both the full aperture extraction and the optimal PSF extraction are calibrated from standard stars observed within the regular *Spitzer* Calibration program. A set of Cohen templates and MARCS code model atmospheres (Decin et al., 2004) provided by the *Spitzer* Science Center[10] are used to derive the spectral response functions. The low resolution full aperture calibration also includes a sample of stars observed within the FEPS legacy program to improve the detailed SRF shape. The low resolution full aperture calibration is discussed in detail in the FEPS Data Explanatory Supplement[11] and will therefore not be discussed in detail in this document.

Only standard stars observed with high accuracy pointing accompanied by dedicated sky observations are used to derive the spectral response function. A complete list of used for the calibration is included in the c2d IRS explanatory supplement. The same procedures used for the science extraction are used for the calibration, but the last stage of flux calibration is omitted. Despite the high accuracy pointing, small pointing errors will be present. To limit the impact of these on the final calibration, the obser-

[10] `http://ssc.spitzer.caltech.edu/irs/calib/templ/`
[11] Available from the SSC FEPS legacy page `http://ssc.spitzer.caltech.edu/legacy/fepshistory.html`

Table 3.2. 1-σ flux calibration uncertainty (%) for high precision pointing

Order	— 1-σ uncertainty —			
	SL[a]	LL[a]	SH	LH
1	5.2	2.8	...	...
2	4.2	4.6	...	...
3	4.2	4.6	...	...
11	...	...	1.0	0.9
12	...	...	1.1	0.9
13	...	...	1.1	0.8
14	...	...	1.1	0.7
15	...	...	1.1	0.7
16	...	...	1.5	0.7
17	...	...	1.5	1.0
18	...	...	1.1	1.0
19	...	...	1.0	1.0
20	...	...	0.9	0.9

[a]The SL uncertainties are dominated by pointing error, the LL uncertainties by the low signal of the standard stars.

vations are sorted by signal strength and the observations from the weakest quarter (assumed to be the sources with the most extreme pointing error) are excluded.

For the optimal PSF extraction, the derivation of the SRF and the PSF parameters are intimately coupled. The derivation is done in steps. In the first iteration, the PSF function is characterized and then, in the second iteration, this PSF function is used in the extraction of the 1-D spectra used to derive the SRFs.

Figure 3.6 shows the derived SRFs and errors for SH and LH modules. The SRF errors depict the point-to-point uncertainty. Table 3.2 lists the average absolute flux calibration uncertainty per order and module for high precision pointing observations.

3.2.5 Error propagation

In the c2d spectral extraction procedure an error is calculated for each spectral data point. This error is propagated in each step of the c2d pipeline and includes the relative spectral response uncertainty (Figure 3.6), the absolute flux calibration uncertainty for high precision pointing (Table 3.2), and, for the full aperture extraction, the deviation between the dither positions. The archival data products delivered through the *Spitzer* Science Center do not contain fully propagated and usable errors (up to pipeline version S14) and are therefore not included. Full error propagation for the SSC pipeline is foreseen for S15, beyond the lifetime of the c2d legacy program.

The c2d extraction error is estimated from the residuals of the profile fit to the observed (source+sky) signal. The profile fitting is performed using the CURFIT routine provided by the OSIA package, which uses a non-linear least squares fit. The error is estimated from the fit residuals,

$$e_{\rm signal}(\lambda) = \sqrt{\frac{\sum_{i=1}^{\rm n}(signal(i) - fit(i))^2}{\rm n \times (n-1)}},$$

where $e_{\rm signal}(\lambda)$ is the estimated extraction error for a given wavelength λ. $signal(i)$ is the observed source+sky signal for a RSC image pixel, $fit(i)$ is the fitted PSF profile plus extended emission, and $\rm n$ the number of good pixels in the aperture for the given wavelength λ as defined in the SSC `wavesamp` calibration file.

After the extraction, the absolute flux calibration and the SRF are applied to the signal and sky estimate. Then the SRF error (e_{SRF}) and the absolute flux calibration uncertainty (e_F) are added to the extraction error;

$$e_{\rm flux}(\lambda) = \sqrt{e_{\rm signal}(\lambda)^2 + \frac{signal^2(\lambda) * (e_{SRF}^2(\lambda) + e_F^2(\lambda))}{SRF^2(\lambda)}}.$$

The absolute flux uncertainty is valid for observations obtained with high precision pointing. For observations obtained with lower accuracy peakup or no peakup, the absolute flux uncertainty can be larger, see Figure 3.12 and § 3.3.4. The pointing error is a few % for the long wavelength modules and may be up to 20% for the SL module which as a result of its narrow beam suffers most from pointing errors.

For the full aperture extraction both dither position are averaged using a weighted mean with $1/e_{\rm flux}^2(\lambda)$ as weights. At each wavelength the absolute difference of the flux in both dither positions is included in the final error.

3.2.6 Defringing

The fringes in IRS originate between plane-parallel surfaces in the light path of the instrument. These surfaces act as Fabry-Pérot etalons, each of which can add unique fringe components to the source signal. The major components in SH and LH originate from the detector substrates. The LL1 fringes are believed to be the result of a filter de-lamination discovered prior to launch. The SL data and LL2 data do not contain any identified fringe residuals.

The fringes observed in the final spectra are residuals of the observed fringes after flux calibration. The observed fringe spectrum is modified during calibration due to wavelength shifts resulting from pointing offsets or a complex source morphology within the slit. No application of a response function (be it the SRFs used in the c2d extractions or the flat field in the SSC BCD extraction) can therefore fully correct for these effects and small residual fringes will be present in most spectra. The amplitudes of the fringe residuals can be up to ∼5% and depend on source morphology, pointing, order, and wavelength.

After extraction and flux calibration, the high resolution (SH and LH) and the LL order 1 spectra are defringed using the IRSFRINGE package developed by the c2d team. The IRSFRINGE documentation and software can be downloaded from the *Spitzer* Post-BCD website.[12] Also see Lahuis & Boogert (2003) for an introduction to IRS defringing.

IRSFRINGE uses a fringe model based on robust sine-wave fitting to remove fringe-residuals from the spectra. Figure 3.7 gives an illustration on how the defringing works

[12] `http://ssc.spitzer.caltech.edu/postbcd/irsfringe.html`

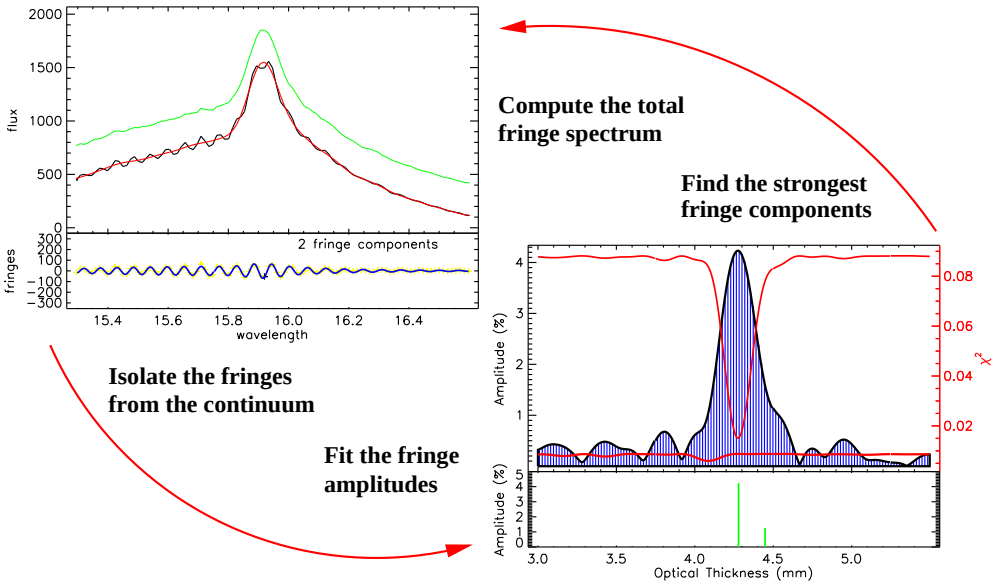

Figure 3.7 Defringing IRS spectra in practice. The left figure shows the original spectrum with the continuum overplotted. The final defringed spectrum is shown offset for clarity. In the lower panel, the continuum subtracted data and the computed fringe spectrum are plotted. In the right figure, the derived fringe amplitude and the effective decrease in chi-squared are plotted for the selected range of optical thickness. In the lower panel, the selected fringe components are shown.

(see also Lahuis & Boogert, 2003). To avoid overfitting, a conservative signal-to-noise cutoff is used in the defringing. This means that residual fringing can still be present in the delivered data and for specific science applications manual defringing may be required on all or part of the spectra.

3.2.7 Order matching

In order to produce cleaner spectra for the SH and LH modules, orders within each module are scaled in flux such that consecutive overlapping orders are matched. For SL and LL this is not done as order mismatches for these modules can be useful for assessing pointing errors. In the wavelength overlap region between SL and LL order 1 and 3 the impact of pointing is different. This difference is reflected in the observed flux loss.

First, the average wavelength and flux are determined from the data of all order overlap regions. These are used as the reference wavelengths and fluxes. The average wavelength and flux for each order in the order overlap regions is then determined for both sides of the order. The orders are finally corrected to the reference using a first order polynomial. For the first and the last order, only a single weighted wavelength and flux is calculated and a zero order correction is applied. The correction is made by scaling the flux of the order, unless the correction slope becomes negative within the order wavelength range, in which case the correction is made by adding/subtracting a

flux offset. This happen for a small number of very weak sources and in a few cases for orders where the flux becomes almost zero due to a very deep silicate 9.8μm absorption band.

To enable an evaluation of the consistency of the spectral slope in the inter-order regions, order clipping is not applied. For example, a slope discontinuity may be a signature that features have been introduced after order matching due to order tilts. This and other spectral artifacts will be discussed in detail in § 3.3.5.

3.3 Data products of IRS pointed observations

For all pointed IRS observations three products are generated:

1. A spectrum for each IRS target as a NASA/IPAC ascii table.
2. Two PostScript files for each spectrum.
   a. PostScript file with the spectrum and extended emission estimate.
   b. PostScript file with the optimized source spectrum, see § 3.3.4.
3. A log file describing each observation (see Appendix A for an example).

A complete overview of all observations is included in the c2d IRS explanatory supplement. The following subsections describe the data products and how they can be used.

3.3.1 IRS c2d products

The IRS pipeline, calibration, and extraction procedures remain in a state of constant development. As a result, the most optimum end-to-end reduction for any observation depends on various parameters that are currently not yet fully understood. In any extracted spectrum, artifacts will be present at some level. Therefore, we employ a number of extraction methods in our reduction pipeline and deliver two spectra for each source.

The c2d observations consist primarily of single staring-mode observations. Since the majority of the sources lie in complex star forming regions, no individual sky observations were taken. For this reason, none of the spectra have been corrected using direct measurements of the local sky. An estimate of the local sky contribution (as estimated in the c2d optimal PSF extraction, see § 3.2.2) is therefore calculated and included in the delivered products. Also a best estimate source spectrum with extended emission and pointing corrections applied is included (see § 3.3.4). An example is given in Figure 3.8.

The products delivered to the SSC include an IPAC format ASCII table that contains the combined 1-D spectra extracted from all observed modules and log files that briefly describe each observation. Included in the log file is a list of the most prominent spectral features (see § 3.3.9). For a first impression, a PostScript plot of the combined spectrum has been generated for each target.

The IPAC tables can easily be read into an IDL data structure within IRSFRINGE or SMART using the command

STRUCT = IPAC2IRS('YOUR_FAVOURITE_SOURCE.TBL').

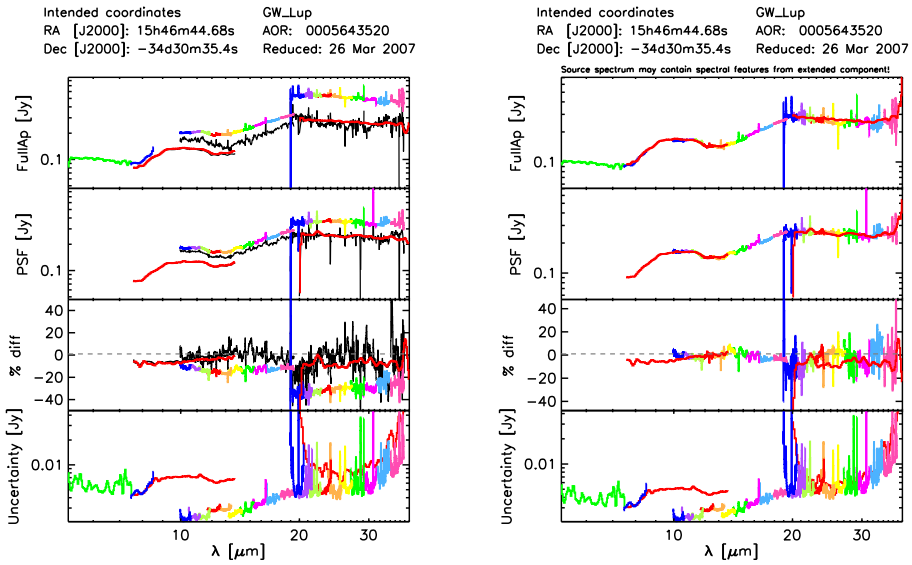

Figure 3.8 PostScript plots provided with the delivered spectra. Left: the extracted IRS spectra. Right: the final optimized source spectrum with an SED correction for the extended emission and a pointing correction to correct for module discontinuities. Shown from top to bottom are, (i) the full aperture extraction, (ii) the PSF extraction, (iii) the relative difference between Fullap and PSF, and (iv) the propagated errors. No error is yet assigned in the extended emission correction and no reverse error correction is applied in the pointing error correction. This source illustrates two issues with IRS spectral data: extended emission and pointing errors. The observed spectra show a strong offset of LH with respect to SH and LL, and of SH with respect to SL. After correcting for extended emission in SH and LH, both match. The discontinuity between SL1 and SL2 and SL1 and SH indicate a pointing error for SL; this is corrected for in the right plot (see § 3.3.4). Note that the final optimized spectra may still contain artifacts, see § 3.3.5 for more details and examples.

The log files include a summary of the source nomenclature and coordinates along with the observation date, mode, and integration times, basic source parameters and identified spectral features. Appendix A gives an example of one of the log files.

The PostScript plots give a quicklook overview of the spectra contained in the data files. Figure 3.8 shows an example of the two plots delivered for each observation.

3.3.2 Source parameters

Basic source characteristics, including the source size (after correction for the PSF size) and location within the slit, are determined within the PSF extraction. These are listed in the log file.

The source size is determined from the width of the PSF function fitted to the source compared to the width of the PSF function fit to standard calibrator stars. A source size of zero implies the source is not extended ($<$ few″) to the *Spitzer* IRS instrument. For staring observations, cross-dispersion positions for both dither positions are deter-

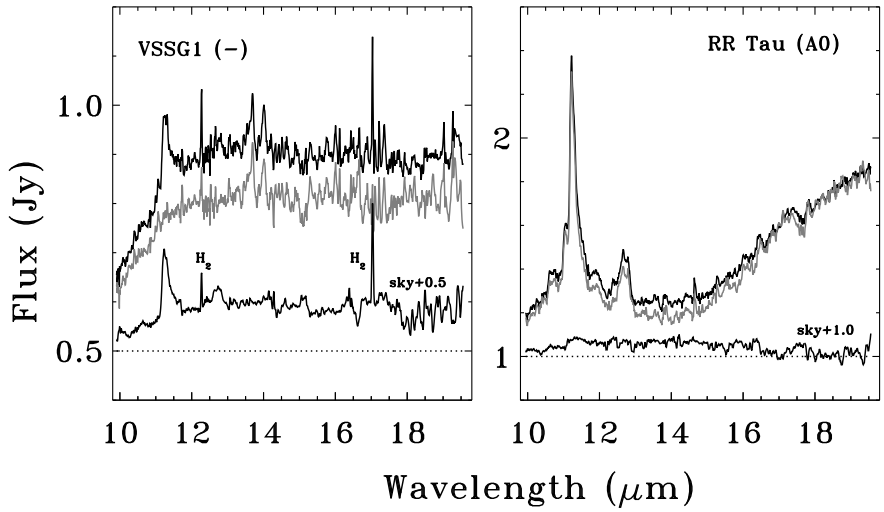

Figure 3.9 Example using the estimate of the local extended emission in the study of PAH spectral features. Shown are the observed spectra and estimated sky emission in black and the sky corrected spectrum in gray. Toward VSSG1, all PAH emission is extended and no PAH intrinsic to the source is observed. Toward RR Tau, all PAH emission is local to the source without confusion by extended emission in the IRS aperture. (Geers et al., 2006).

mined for all modules. The offset listed in the log file is the offset with respect to the average cross-dispersion positions for the sample of standard stars which have been observed with high accuracy peak-up. The cross dispersion offsets can be used as a first order estimate of the dispersion offset, and thereby the flux loss, of the orthogonal slits. This means the LH cross dispersion offset gives an estimate for the SH dispersion offset and vice versa. The same applies to the SL and LL modules.

3.3.3 Extended emission

The optimal PSF extraction and the full aperture extraction for the SL1, LL1, SH, and LH modules provide a direct measure of the amplitude of the zero level of the spectrum. This zero level is a combination of extended emission in the direct vicinity of the source, be it sky or envelope emission, and residuals of, e.g., the dark current subtraction in the SSC pipeline. For the full aperture extraction, the extended emission is estimated from the PSF extraction scaled to the full aperture size. Though for SL1 and LL1 a sky correction derived from the other dither position is applied, extended emission can still be present, e.g. as a result of incorrect straylight correction for SL1 or because the extended sky emission varies strongly over the grid.

The flux values delivered in the c2d products contain the signal of the source plus the extended emission. For the full aperture extraction the flux is in units of Jy/Aperture and for the PSF extraction it is in Jy/beam. Thus, for a point source without extended emission, this flux is in Jy.

It is possible to spot extended spectral features in the spectra in two ways. The first one is to directly subtract the estimated extended emission of the observed spectrum,

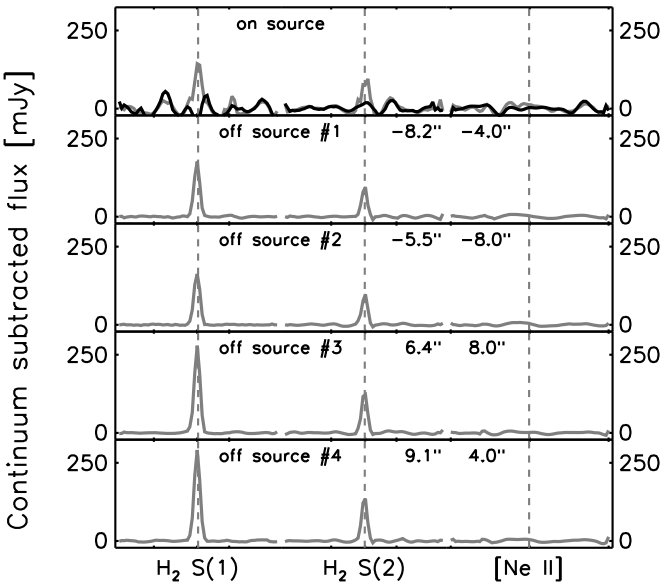

Figure 3.10 Example of extended molecular hydrogen line emission toward VSSG 1. Plotted in gray is the total observed emission. Plotted in black in the top panel is the emission after the estimated extended component is subtrated. This illustrates the problem of detecting unresolved emission toward young stars; the extended emission is often significantly stronger than the unresolved source component and can vary with position. In this example, no compact on-source emission has been detected.

see Figures 3.9 and 3.10 for examples. The second way is to compare the peak strength of the feature. For extended features, the peak strength in the full aperture extraction will be stronger than in the PSF extraction reflecting the difference in aperture ($\sim 10 - 12\,\mathrm{pixel}^2$) versus beam ($\sim 3 - 5\,\mathrm{pixel}^2$), see e.g. the H_2 S(1) emission line presented in Figure 3.13.

The estimate of the extended emission is, by nature of the fitting process, inherently more noisy and uncertain than the total signal. Therefore no automated correction is applied but it is left to the user to use the extended emission estimate. When used for SED analysis or the study of resolved features, a smoothed version of the extended emission spectrum can be used which does not introduce spectral noise (e.g., see studies of extended PAH emission by Geers et al. (2006) and the example in Figure 3.9). When analyzing unresolved features (e.g., studies of H_2 emission lines by Lahuis et al. (2007) and the example in Figure 3.10), a direct subtraction of the extended emission or a correction of a Gaussian line fit to the extended emission is required to obtain the unresolved source component.

3.3.4 Final source spectrum

In order to provide the most useful products that reflect more closely the on-source emission, additional corrections are applied to the results of the Fullap and PSF extractions (see Figures 3.11 and 3.8 for an example). First for SL1, LL1, SH, and LH the

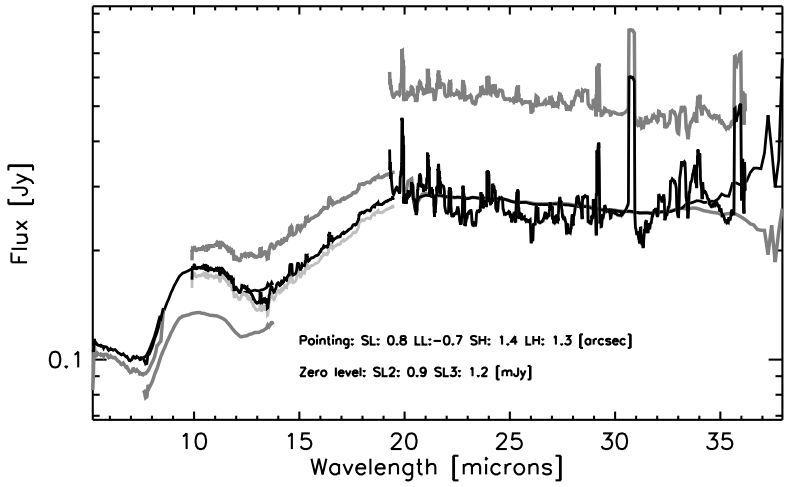

Figure 3.11 Producing a final spectrum for the source GW Lup which has both extended emission and a pointing offset. In dark gray the observed signal (Fullap), in light gray the signal of SH and LH corrected for extended emission, and in black the final spectrum (see § 3.3.4 for details). Note that light gray and black for LH are virtually on top of each other. The optimum pointing offsets and zero level corrections are printed below the spectrum. Note that the final spectra often still contain artifacts, in particular the LH module, see § 3.3.5 for more details and examples. The pointing correction was done using a β-version of the pointing fluxloss calibration and software, a collaborative effort of the c2d and FEPS legacy teams.

estimated extended emission component (see § 3.3.3) is subtracted. After this, pointing errors are corrected based on optimal module matching. The optimization is done by minimizing the difference between the modules (see Table 3.1) over the complete overlap range to maximally exploit the strong wavelength dependence of the fluxloss functions (see Figure 3.12). The module overlap regions of SL2/SL1, SL1/SH, SH/LH, LL2/LL1, and LL/SH+LH are used.

Since the extended emission estimates inherently contain more noise and artifacts than the complete (source+extended emission) spectrum, a smoothed version over the complete module wavelength range is subtracted from the observed spectrum. The extended emission estimates are smoothed with a broad median filter and then fit with a low order polynomial (4th order for low resolution and 6th order for high resolution). To suppress edge effects the spectra are padded with the smoothed flux on both wavelength ends. For the low resolution modules, an extended emission correction is applied during extraction. Residual extended emission can still be present as a result of, e.g., a varying local sky, SL straylight residuals, or dark current residuals. For SL1 and LL1, the extended emission estimate is used for the correction, but this is not usable for SL and LL order 2 and 3. Instead, for these orders, an additional zero level correction is included in the module optimization.

If for a particular module *no* unresolved (or slightly extended) source component could be identified during extraction, the final source spectrum is set to zero for that module. For example, an extremely blue or extremely red object may have no detectable source signal in only the long or short wavelength modules, respectively. If the

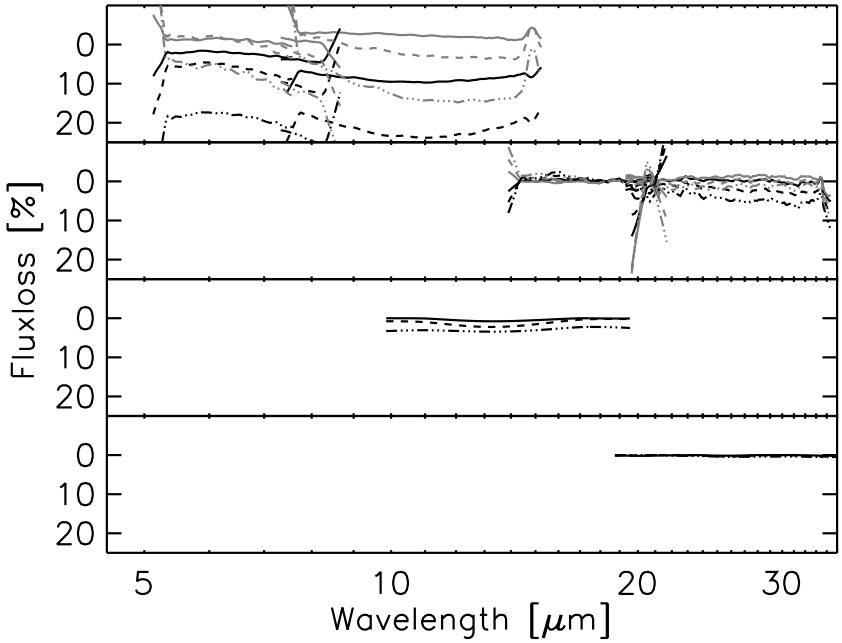

Figure 3.12 Pointing error flux loss for 0.4, 0.8, and $1.2''$. The SL and LL fluxloss functions are derived from standard star mapping observations, the SH and LH fluxloss functions are derived from the optimal extraction cross dispersion PSF assuming a spherical PSF. Empirical fluxloss functions for SH and LH are to be derived at a later date. For SL and LL it should be noted that the PSF is not centered on the slit and two curves are plot for each offset, for a positive and a negative pointing error. The characterization of the pointing fluxloss is a collaborative effort of the c2d and FEPS legacy teams.

source is fully extended in all modules, then the source spectrum contains the original spectrum without correction.

The pointing offsets (in arcseconds) and zero level offsets (in Jy) required to optimally match the modules in the spectra are listed in the IPAC table header. The pointing offset estimates are listed using the keywords SLPE_PSF (pointing offset for PSF spectrum), SLPE_SRF (pointing offset for FullAp spectrum) and similar for the other modules. The SL and LL zero level offsets are included in the header using SL2Z_PSF (SL order 2 zero level for PSF spectrum), and similar for order 3, the FullAp extraction (_SRF), and the LL modules (see Appendix B).

It should be noted that only a smoothed low resolution correction for the extended emission is applied. Therefor spatially extended unresolved spectral features, such as H_2 or forbidden line emission, are not removed from the final spectra. If extended spectral features are present, then a careful examination of the original spectrum and estimated extended emission (see § 3.3.3) is required in order to use the spectra for science analysis.

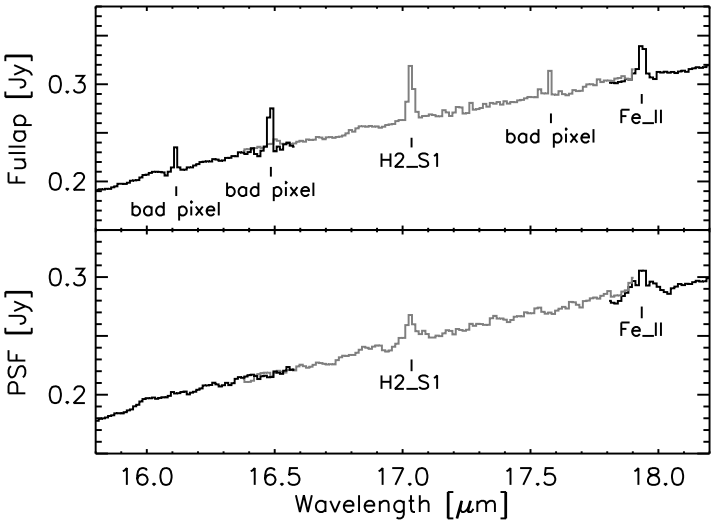

Figure 3.13 Example of a source spectrum (Sz 102) with bad pixels and gas-phase features. In this region of the spectrum, there are clearly identified bad pixels (near 16.1 and 17.6 μm), one multi-pixel spike near 16.5 μm, and strong multi-pixel gas phase lines (H2_S1 at 17.04 μm and Fe_II at 17.9 μm). Comparing the two spectra helps to identify the bad pixels. Note the difference in the strength of the H_2 S(1) and [Fe],II] lines between the extractions as a result of the line emission being extended while the continuum emission comes from the unresolved source.

3.3.5 IRS artifacts

As noted above, the c2d correction of bad/hot pixels, as well as pixels flagged in the BCD pipeline, greatly improves the final S/N ratio of the spectra. This does not mean, however, that the spectra are free of artifacts. The inclusion of spectra extracted using two different extraction techniques can be used to recognize the presence of some artifacts, but this is not guaranteed to be foolproof. Artifacts, both resolved and unresolved, can be present in the delivered spectra and great care should be taken when interpreting any "features."

Therefore, we will now discuss various types of artifacts that we have found to be present in the c2d spectra. This list is not meant to be all-inclusive, but should be viewed as examples of the types of artifacts that are most common. These artifacts may arise from a variety of factors.

3.3.6 Spikes

Narrow (1–2 pixel wide) spikes in the spectrum can often be associated with 'hot' or bad pixels that were not identified and corrected using the interpolation routines (see § 3.2.1 and Figures 3.2 and 3.3). As discussed above, these artifacts are most prominent in the LH spectra, but they also appear in the LL, SH, and, occasionally, SL modules. The PSF and Fullap extractions use different methods to correct for bad pixels; for the Fullap method, the pipeline finds and interpolates bad pixels prior to extraction and

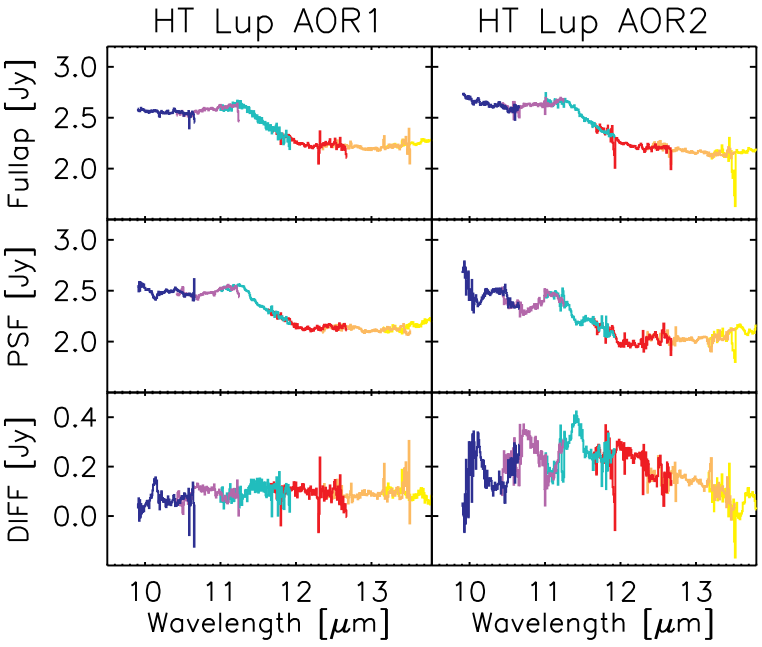

Figure 3.14 Extracted spectra for HT Lup AOR1 (IRS staring mode, left) and AOR2 (IRS mapping mode, right) are shown. The differences in the shapes of the lowest wavelength SH orders (where the spatial sampling to which the PSF extraction is sensitive becomes critical) between the extractions exemplifies order curvature type artifacts. The AOR2 spectrum shows that the PSF extraction becomes less reliable when used for the spectral extraction from single map pointings as a result of the narrower cross dispersion baseline compared to wider baseline in the combined two dither positions for the staring observation. Note that due to the order curvature artifacts, the user must be careful when interpreting the shape of the amorphous silicate 10 μm feature and/or the identification of crystalline forsterite or PAH features (both near 11.3 μm). In the case of HT Lup, we are fortunate to have 2 different observations to compare, in most cases, one must use the error estimates and comparisons of PSF vs. Fullap extractions to determine whether order curvature is a factor.

the PSF method only includes pixels identified as "good" in the extraction. Therefore, comparing the resulting spectra from the two extractions can often help to identify bad pixels (see Figure 3.13), as they may appear in only one spectrum. Additionally, true gas-phase lines will usually be a bit broader (2-3 pixels wide) than spikes due to bad pixels, but it is often difficult to distinguish real emission and (1–2 pixel wide) spikes should always be treated with caution.

3.3.7 Edge effects

Artifacts located at the edges of orders may be present due to "order curvature," "order tilt," or "bad order matching" (that is, there can sometimes be large differences in flux or spectral shape between successive orders). Such problems often arise when the source is not centered in the slit. The PSF correction applied to both full slit and

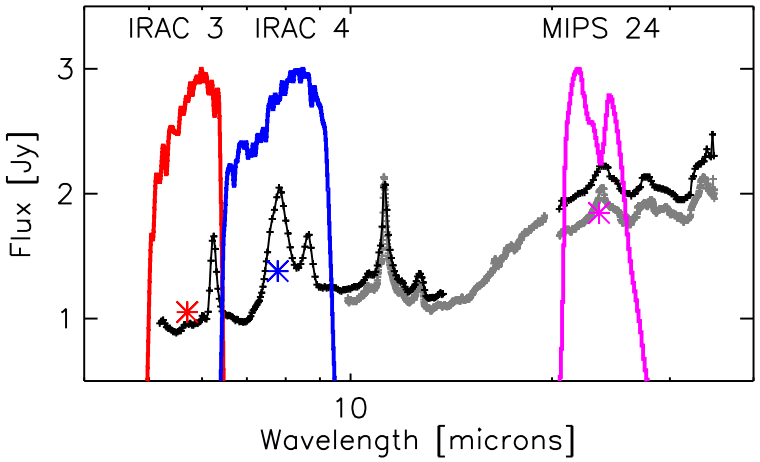

Figure 3.15 The observed *Spitzer* IRS spectrum of RR_Tau and the IRAC 3, IRAC 4, and MIPS 24 filter profiles used to derive the continuum values together with the feature identification. In grey are the SH and LH spectra and in black the SL and LL spectra.

source profile fitting extractions has reduced the frequency and severity of these types of artifacts, but they are still often present, and are particularly common in cases with large pointing offsets. Order curvature often results in "V" shaped dips or increases in the flux of the spectrum at the intersection of two orders. These can easily be misinterpreted as solid-state emission or absorption features (See Figure 3.14). Order tilt in successive orders, if corrected by scaling the orders to match in the overlap regions, can result in an increase in the continuum slope in the affected spectral region. If left uncorrected, order tilts or bad order matches result in sharp jumps in the spectrum in the order overlap region. In most cases, one must use the error estimates and comparisons of PSF vs. Fullap extractions to determine whether order curvature is an artifact. If the log file indicates that there is a pointing offset, order artifacts will likely be corrected in the final pointing corrected source spectrum.

3.3.8 Module mismatches

Additionally, there may be significant differences in the flux of consecutive modules (see Figure 3.11). This is particularly true in the overlap between high resolution and low resolution modules, particularly for the full slit extraction, due to differing contributions from background flux. Pointing offsets will also result in flux differences between modules, as the module slits are oriented perpendicular to one another. Again, if these issues are due to pointing offsets, then they should be corrected in the final source spectrum.

3.3.9 Spectral features

To provide a quick assessment of the nature of the observed sources, an automated feature identification, restricted to a selected set of spectral features (see Table 3.3), is included in the c2d pipeline. The identified features for each source are listed in the

log files (Appendix A) and complete lists of features found in all sources are presented in the c2d explanatory supplement. In these the integrated fluxes of the IRS spectra over the IRAC 3, IRAC 4, and MIPS 24 photometric bands using the instrumental filter profiles (see Figure 3.15 for an example) are also included. The feature tables have been checked by eye by c2d team members and comments (about suspect features, etc.) are noted in the logs. Given the complexity of the data and the observed features (e.g., the presence of extended emission and pointing uncertainties), no feature strengths or optical depths are derived. To do so requires more sophisticated fitting procedures.

In order to reduce the mis-identification of features the extended emission and pointing corrected spectra (see § 3.3.4) are used as input for the feature identification. Remaining offsets between consecutive modules are corrected such that the overlapping regions match in flux. The modules are matched pairwise, SL1 to SH, SL2 to SL1, LH to SH, and LL to combined data from SH and LH. This additional module matching is only done to facilitate the feature ID process. As mentioned in § 3.3.5, the difference in flux between modules is likely due to differences in background emission and/or pointing offsets. Simply scaling the modules may not be the correct approach for determining the strength or composition of features, but is acceptable for determining the *presence* of the strongest, most easily identified features, as done here.

Feature identification

Table 3.3 lists the feature information and constraints used by the feature identification script. The wavelength (λ) and FWHM are used to initialize the fit parameters of the feature profile and are allowed to vary within a limited range ($\sim$0.3$\times$FWHM). The continuum points define two regions on either side of the feature, one on the short wavelength side (between wavelengths cont 1a and cont 1b) and one on the long wavelength side (between cont 2a and cont 2b). These continuum regions are used to make an initial estimate of the continuum parameters. After parameter initialization, a Gaussian profile with a 2nd order polynomial is fitted to the data between cont 1a and cont 2b. When two values are listed for λ and FWHM in Table 3.3, a two component Gaussian fit is made. This is the case for overlapping features, e.g., ICE_6 and PAH_7_8, and for features with shapes that are non-Gaussian and require a multiple component fit, e.g, for CO_2, SiO_s, and SiO_b. Though a simple two-component fit is insufficient to accurately reproduce the shape of the latter bands, it is sufficient to establish their presence or absence.

Narrow lines

A number of gas-phase emission lines are searched for by the feature identification program. This includes all molecular hydrogen lines in the IRS range, from H_2 S(0) to H_2 S(7), and a number of atomic forbidden lines. As these lines are expected to be unresolved, the FWHM is set to the instrument resolution and wavelengths to determine the continuum are set to the following, cont 1a=-4$\times$FWHM, cont 1b=-1.5$\times$FWHM, cont 2a =1.5$\times$FWHM, and cont 2b=4$\times$FWHM. For all lines, a Gaussian profile with a center position and a width are fit to within 25% of the instrument resolution. A larger offset in the center position is not acceptable considering the accuracy of the IRS wavelength calibration.

Table 3.3. Input list for automatic feature identification

ID	em/abs/cnt	λ[a] [μm]	FWHM[b] [μm]	cont 1a[c] [μm]	cont 1b[c] [μm]	cont 2a[c] [μm]	cont 2b[c] [μm]
H2_S0	em	28.219	...	...	...	...	...
H2_S1	em	17.035	...	...	...	...	...
H2_S2	em	12.279	...	...	...	...	...
H2_S3	em	9.665	...	...	...	...	...
H2_S4	em	8.025	...	...	...	...	...
H2_S5	em	6.91	...	...	...	...	...
H2_S6	em	6.109	...	...	...	...	...
H2_S7	em	5.511	...	...	...	...	...
Ne_II	em	12.814	...	...	...	...	...
Ne_III	em	15.56	...	...	...	...	...
Fe_I	em	24.042	...	...	...	...	...
Fe_II	em	17.936	...	...	...	...	...
Fe_II	em	25.988	...	...	...	...	...
S_I	em	25.249	...	...	...	...	...
S_III	em	18.71	...	...	...	...	...
Si_II	em	34.82	...	...	...	...	...
PAH_11.3	em	11.3	0.1	10.5	10.9	11.6	12.1
PAH_12	em	12.7	0.3	11.9	12.3	13.0	13.6
PAH_6	em	6.2	0.2	5.7	6.05	6.5	6.8
PAH_7_8	em	7.7 & 8.6	0.7 & 0.4	6.8	7.10	9.0	9.3
CO_2	abs	15.15& 15.5	0.35 & 0.5	14.40	14.75	15.87	16.39
ICE_6	abs	6.0 & 6.85	0.4 & 0.3	5.40	5.65	7.20	7.60
SiO_s	abs/em	9.7 & 11.0	1.5 & 1.5	7.1	7.9	13.0	14.0
SiO_b	abs/em	18.52 & 22.0	3.0 & 3.0	13.2	14.7	25.	30.
SiO_l	em	34.0	2.0	30.5	31.5	36.0	37.5
Em_11.3	em	11.3	0.6	10	10.7	11.7	12.5
IRAC 3	cnt	5.7	...	...	...	...	...
IRAC 4	cnt	7.8	...	...	...	...	...
MIPS 24	cnt	23.5	...	...	...	...	...

[a] The center wavelength of the Gaussian fitting profile. When two wavelengths are listed, the fitting profile is composed of two Gaussian components.

[b] The full width at half maximum of the Gaussian fitting profile. When two FWHM are listed, the fitting profile is composed of two Gaussian components.

[c] The continuum is defined as from cont 1a to cont 1b on the short wavelength side of the feature and from cont 2a to cont 2b on the long wavelength side of the feature. — If the FWHM and continuum wavelengths are not defined, then the feature is either unresolved or a continuum feature. For unresolved features, the FWHM is set to the instrument resolution and the continuum regions are defined as; cont 1a= $\lambda - 4\times$FWHM, cont 1b= $\lambda - 1.5\times$FWHM, cont 2a= $\lambda + 1.5\times$FWHM, and cont 2b= $\lambda + 4\times$FWHM.

Note. — For the continuum features, IRAC 3, IRAC 4, and MIPS 24, the instrumental filter profiles are used (see Figure 3.15).

PAH features

The most prominent features from polycyclic aromatic hydrocarbons (PAHs), near 6.2, 7.7, 8.6, 11.3 and 12.7 μm, are included in the c2d feature identification. The 6.2 and 12.7 μm features are fairly isolated, but the 7.5 and 8.6 μm features overlap with each other and the 11.3 μm feature overlaps with the broad 9.8 μm silicate feature. For this reason, the feature ID program groups the 7.5 and 8.6 features together as "PAH_7_8," fitting a profile that is the combination of two Gaussian profiles. The feature fit for the 11.3 μm feature uses the underlying silicate feature as the "continuum" looking for a narrow feature with a width of $<$0.2 μm. PAH features, when identified, are subtracted from the spectrum before silicate features are fit.

Silicate bands

The c2d feature identification program searches for the most prominent silicate features, which are broad amorphous olivine/pyroxene Si-O stretching and O-Si-O bending modes, in emission or absorption, at 9.8 and 18 μm (labeled "SiO_s" and "SiO_b"), and a crystalline silicate (forsterite/enstatite) lattice mode emission feature at 33–35 μm ("SiO_l"). There are several crystalline silicate emission features overlapping with the broad amorphous features, but the exact wavelengths of these features are dependent on the grain size and composition (Kessler-Silacci et al., 2006). They are difficult to be reliably identified in this automated method and are therefore not included. The one exception is a crystalline forsterite feature near 11.3 μm, which often can be distinguished from the 9.8 μm amorphous feature. However, this feature overlaps with the narrow 11.3 μm PAH feature, but appears to be broader in sources with verified crystalline silicates. For this reason, in cases where a feature can be identified near 11.3 μm, but the feature is broader (width $\sim$0.6 μm) than typically seen for PAH, we label it as "Em_11.3." In some cases, identification of Em_11.3 could be due to an SiO_s feature with a flattened shape, possibly indicative of grain growth. Detailed compositional modeling of the spectra are required to determine if this feature is due to PAH or forsterite emission. The identification of the broad amorphous SiO_s and SiO_b features can sometimes be confused by the presence of strong, narrow crystalline silicate emission features. In addition, for a number of observations, SL order 1 data is not available, thus cutting off a part of the SiO_s feature. In some cases this may lead to a non-detection or a false detection.

Ices

There are several ice absorption features, but the c2d feature identification includes only the most prominent: the CO_2 feature near 15.1 μm and two overlapping ice features near 6.0 and 6.85 μm (combined as "ICE_6").

Blended features

Several features in the spectra are blended with other features, e.g. H_2 emission lines on top of the ICE_6 band, PAH 11.3 μm emission on top of a Si-O stretching mode band, and CO_2 absorption on the very broad Si-O bending mode profile. For this reason, a feature is removed from the spectrum (only for the purposes of feature identification) after it has been positively identified.

Identified feature tables

Complete lists of features identified in the observed spectra are presented in the c2d IRS explanatory supplement. The first table lists the detection status for all gas phase molecular hydrogen and atomic lines and the second table lists the detection status for all solid-state features, including features from PAHs, ices, and silicates. Also listed, in the last 3 columns of second table, are the spectral fluxes integrated over the IRAC 3, IRAC 4, and MIPS 24 photometric bands. In both tables, a check mark (✓) denotes that the feature has been detected at $> 5\sigma$, averaged for both the full slit and source profile fitting extractions, and at least 3σ in both extractions. For the 9.8 and 18 μm silicate

bands, "✓(A)" and "✓(E)" denote that the feature was detected in absorption or emission, respectively. A question mark (?) denotes that the feature has been detected at $3-5\sigma$ in amplitude, averaged for both the full slit and source profile fitting extractions. Dashes ("-") indicate non-detections. These tables can be used to get an overview of the most prominent features in each spectrum, but should not be considered as a complete or definitive inventory. In the case of extended emission, for example, the PSF extraction will show a much weaker feature than the full aperture extraction, and thus the feature may not meet the above criteria. In cases where the feature identifications made by the automated routine are determined by visual inspection to be incorrect or questionable, a note is made in the log file and in the tables, but the feature is still listed.

It should also be noted that many of the observed emission lines and several PAH features are resulting from extended emission close to the source (§ 3.3.3). Therefore, the features identified in the spectrum and attributed to a particular target in the tables and logfiles may not be due to on-source emission. For a number of these extended emission lines (Lahuis, in prep.) and PAH features (Geers et al., 2006) no source emission or only a (weak) source component is found by carefully using the sky estimate derived from the optimal PSF extraction.

3.4 Summary

This chapter describes the c2d reduction pipeline and the products it generates. This pipeline is used to generate the products used for the science analysis by the c2d team members (such as IRS data used in this thesis) and the products included in the final legacy data delivery of improved products to the *Spitzer* Science Center. It describes, in considerable detail, the products and the algorithms and calibration products used to derive them. The delivery consists for the most part of IRS staring observations, but also includes some MIPS SED and IRS mapping observations, however this Chapter focusses on the reduction of the IRS staring observations. The generated products include data tables, illustrative plots and informative logfiles.

Appendix A – IRS observation logfile

Logfile for the *Spitzer* IRS observation as shown in Figure 3.8.

```
Quality check file for Spitzer/IRS observation.

Source:       GW_Lup
Coordinates:  15h46m44.7s -34d30m35.4s [J2000]
Observer:     Neal Evans, OID 87
Program:      From Molecular Cores to Planets, continued
Obs. date:    2004-08-30
AOR:          0005643520
AOR label:    IRSS-0068
AOT type:     irsstare
Obs. mode:    TargetFixedSingle
Peak up mode: --
IRS Pipeline: S13.2.0
Modules:      SL1, SL2, LL1, SH, LH

The longslit images of the SL2 and LL2 modules are severely undersampled
over most of their wavelength range. As a result the PSF extraction is
unstable for these modules. Therefore the PSF, PSF_sky, and the FullAp_sky
columns contain no data.
============================================================
```

```
Data summary:
-------------
SL integration: 14*1*2 (tint*ndce*nexp)
SH integration: 121*2*2 (tint*ndce*nexp)
LL integration: 14*4*2 (tint*ndce*nexp)
LH integration: 60*4*2 (tint*ndce*nexp)

SL SNR:  20   STDEV:     5 [mJy]
SH SNR:  66   STDEV:     2 [mJy]
LL SNR:  34   STDEV:     7 [mJy]
LH SNR:  49   STDEV:     6 [mJy]

SL source size             :   1.1 [arcsec]
SL X-dispersion offset     :   0.2 [arcsec]
SL pointing offset estimate:   0.8 ...   0.8 [arcsec]
SH source size             :   0.4 [arcsec]
SH X-dispersion offset     :   0.9 [arcsec]
SH pointing offset estimate:  -0.9 ...  -0.6 [arcsec]
LL source size             :   1.9 [arcsec]
LL X-dispersion offset     :   1.0 [arcsec]
LL pointing offset estimate:  -0.9 ...  -0.4 [arcsec]
LH source size             :   0.0 [arcsec]
LH X-dispersion offset     :  -0.5 [arcsec]
LH pointing offset estimate:   1.3 ...   3.2 [arcsec]
============================================================
Most prominant spectral absorption and emission features identified in the
Spitzer/IRS spectrum of GW_Lup

IRAC3, IRAC4, and MIPS24 give the flux of the observed spectra, if possible
with a correction for extended emission and pointing errors, convolved with
the respective passbands.

SNR estimate is the peak intensity or peak optical depth of the feature
over the residual rms after feature fitting.

N.B. The identification is done using an automated script.
     Caution should therefore be taken at all times.

    id      abs=2      lambda [um]     snr
             em=1      lambda [um]     snr
            cnt=-1     lambda [um]   flux [mJy]
SiO_s          1          9.700        17
Em_11.3        1         11.300         5
irac3         -1          5.702        96
irac4         -1          7.784       111
mips24        -1         23.512       264
#> ------------------
- The spectra are good
- Features identification is ok
- Em_11.3 could also be caused by a broad SiOs feature.
```

Appendix B – IRS table header

Header of IRS spectral table for the *Spitzer* IRS observation as shown in Figure 3.8.

```
\c2d_irs_spectrum
\processing date Nov 2006
\char HISTORY ==============
\char HISTORY The spectrum presented in this table is a combination
\char HISTORY of all Spitzer/IRS c2d data for the object GW_Lup
\char HISTORY The data have been observed, reduced and verified by the
\char HISTORY Spitzer c2d legacy team:
\char HISTORY     'From Molecular Cores to Planet Forming Disks'
\char HISTORY          http://peggysue.as.utexas.edu/SIRTF/
\char HISTORY Before using this data please read the quality file accompanying
\char HISTORY this specific dataset and the complete documentation of the
\char HISTORY release of all the c2d legacy data.
\char HISTORY
\char HISTORY For questions please contact the Spitzer helpdesk
```

```
\char HISTORY          help@spitzer.caltech.edu
\char HISTORY who will answer your questions or forward them to one of
\char HISTORY the c2d IRS experts.
\char HISTORY ==============
\char NAXIS   =                    2 / STANDARD FITS FORMAT
\char ORIGIN  = '   c2d Legacy team' / Organization generating this FITS file
\char TELESCOP= '           Spitzer' /
\char INSTRUME= '              IRSX' /
\char EQUINOX = '            2000.0' / Equinox
\char CREATOR = '           S13.2.0' / SSC Pipeline Version
\char OBJECT  = '            GW_Lup' / Target Name
\char RA_HMS  = '      15h46m44.68s' / [hh:mm:ss.ss] Commanded RA as sexagesimal
\char DEC_DMS = '      -34d30m35.4s' / [dd:mm:ss.s] Commanded Dec as sexagesimal
\real RA_SLT  =           236.68617 / [deg] RA at slit center
\real DEC_SLT =           -34.50983 / [deg] DEC at slit center
\char DATE_OBS= '        2004-08-30' / Observation Date
\char AOT_TYPE= '          irsstare' / Observation Template Type
\char OBJTYPE = ' TargetFixedSingle' / Target Type
\char PEAKUP  = '                --' / Peakup
\char AORLABEL= '         IRSS-0068' / AOR Label
\char AORKEY  = '        0005643520' / AOR key. Astrnmy Obs Req Req
\char OBSRVR  = '        Neal Evans' / Observer Name
\char OBSRVRID= '                87' / Observer ID of Principal Investigator
\char PROGID  = '              172' / Program IDe
\char PROTITLE= 'From Molecular Cores to Planets, continued' / Program Title
\real SL_TINT =                14.68 / SL Ramp integration time
\int  SL_NDCE =                    1 / SL Commanded number of DCEs
\int  SL_NEXP =                    2 / SL Number of exposures per DCE
\real SH_TINT =               121.90 / SH Ramp integration time
\int  SH_NDCE =                    2 / SH Commanded number of DCEs
\int  SH_NEXP =                    2 / SH Number of exposures per DCE
\real LL_TINT =                14.68 / LL Ramp integration time
\int  LL_NDCE =                    4 / LL Commanded number of DCEs
\int  LL_NEXP =                    2 / LL Number of exposures per DCE
\real LH_TINT =                60.95 / LH Ramp integration time
\int  LH_NDCE =                    4 / LH Commanded number of DCEs
\int  LH_NEXP =                    2 / LH Number of exposures per DCE
\char SL_SIZE = '              1.1' / SL source size estimate
\char SL_XOFF = '              0.2' / SL cross dispersion offset
\char LL_SIZE = '              1.9' / LL source size estimate
\char LL_XOFF = '              1.0' / LL cross dispersion offset
\char SH_SIZE = '              0.4' / SH source size estimate
\char SH_XOFF = '              0.9' / SH cross dispersion offset
\char LH_SIZE = '              0.0' / LH source size estimate
\char LH_XOFF = '             -0.5' / LH cross dispersion offset
\real SLPE_PSF=                0.77 / SL pointing offset for psf spectrum
\real SLPE_SRF=                0.77 / SL pointing offset for fullap spectrum
\real LLPE_PSF=               -0.86 / LL pointing offset for psf spectrum
\real LLPE_SRF=               -0.42 / LL pointing offset for fullap spectrum
\real SHPE_PSF=               -0.91 / SH pointing offset for psf spectrum
\real SHPE_SRF=               -0.63 / SH pointing offset for fullap spectrum
\real LHPE_PSF=                1.26 / LH pointing offset for psf spectrum
\real LHPE_SRF=                3.20 / LH pointing offset for fullap spectrum
\real SL2Z_SRF=              0.0100 / SL order 2 zero level for fullap spectrum
\real SL3Z_SRF=              0.0100 / SL order 3 zero level for fullap spectrum
\char COMMENT ==============
\char COMMENT The longslit images of the SL2 and LL2 modules are
\char COMMENT severely undersampled over most of their wavelength range.
\char COMMENT As a result the PSF extraction is unstable for these modules.
\char COMMENT Therefore the PSF and the FullAp_sky columns contain no data.
\char COMMENT ==============
\char COMMENT The PSF_SRC and FULLAP_SRC columns contain the observed spectra
\char COMMENT corrected for extended emission within the IRS SH and LH aperture
\char COMMENT and flux loss due to pointing errors.
\char COMMENT Note that the extended emission correction uses a low resolution
\char COMMENT of the estimated sky and the resulting SRC spectrum may therefor
\char COMMENT still contain spectral features (e.g. H2 and PAH) from a
\char COMMENT spatially extended  component.
\char END
```